HHS Public Access

Author manuscript

Nat Cell Biol. Author manuscript; available in PMC 2024 May 28.

Published in final edited form as:

Nat Cell Biol. 2022 June ; 24(6): 815–824. doi:10.1038/s41556-022-00933-9.

Illuminating RNA biology through imaging

Phuong Le[1,2,3], **Noorsher Ahmed**[1,2,3,4], **Gene W. Yeo**[1,2,3,4,✉]

[1]Department of Cellular and Molecular Medicine, University of California San Diego, La Jolla, CA, USA.

[2]Stem Cell Program, University of California San Diego, La Jolla, CA, USA.

[3]Institute for Genomic Medicine, University of California San Diego, La Jolla, CA, USA.

[4]Biomedical Sciences Graduate Program, University of California San Diego, La Jolla, CA, USA.

Abstract

RNA processing plays a central role in accurately transmitting genetic information into functional RNA and protein regulators. To fully appreciate the RNA life-cycle, tools to observe RNA with high spatial and temporal resolution are critical. Here we review recent advances in RNA imaging and highlight how they will propel the field of RNA biology. We discuss current trends in RNA imaging and their potential to elucidate unanswered questions in RNA biology.

The transformation from DNA to protein is a complex, multi-stage process that revolves around RNA metabolism. After transcription, RNA molecules proceed to splicing, localization, translation and degradation. These steps are highly coordinated and tightly regulated in both spatial and temporal domains. Traditional biochemistry and genetic tools have elucidated some of the what and the how, such as the identities and functions of proteins and non-coding RNAs (ncRNAs) involved in each step of RNA processing. To delve deeper into the when and where, methods to visualize RNA within cells are required. Towards this goal, in the past four decades groups have developed and advanced RNA imaging tools for both fixed and live cells (Fig. 1 and Table 1). These RNA imaging tools take advantage of recent and rapid innovation in fluorescent microscopy, image processing, DNA chemistry and next-generation sequencing to achieve multiple milestones, including single-molecule sensitivity, super-resolution, multiplexing and live-cell RNA tracking. In this Review we discuss the developments in RNA imaging and the RNA biology they have and are poised to unravel.

✉**Correspondence** should be addressed to Gene W. Yeo., geneyeo@ucsd.edu.

Competing interests

G.W.Y. is a SAB member of Jumpcode Genomics and a co-founder, member of the Board of Directors, scientific advisor, equity holder and paid consultant for Locanabio and Eclipse BioInnovations. G.W.Y. is a visiting professor at the National University of Singapore. G.W.Y.'s interests have been reviewed and approved by the University of California San Diego, in accordance with its conflict-of-interest policies. The authors declare no other competing interests.

RNA imaging technologies

RNA imaging technologies have been evolving rapidly for both fixed and live cells. In fixed cells, current methods have achieved substantial throughput and are capable of detecting localization and quantifying the expression level of the whole transcriptome. In live cells, throughput is limited to a single gene per colour; however, the temporal resolution of live-cell RNA imaging has significantly advanced our understanding of the dynamics of RNA processing.

Fixed cells and fluorescence in situ hybridization

In 1982, Singer and Ward were among the first to demonstrate fluorescence in situ hybridization (FISH) for RNA detection by probing actin messenger RNA (mRNA) with rhodamine-conjugated avidin binding to a DNA probe with incorporated biotinylated 2′-deoxyuridine-5′-triphosphate (dUTP)[1]. In 1998, single-molecule FISH (smFISH) was developed using a complementary DNA (cDNA) oligonucleotide synthesized with five fluorochromes per probe[2]. In 2008, the method was further refined to detect mRNAs at single-molecule resolution by probing each mRNA with 48 DNA probes, each labelled with single fluorochromes[3]. Rather than tiling multiple probes to a desired mRNA target, rolling-circle amplification (RCA)-FISH first hybridizes and ligates a padlock probe specific to the mRNA target and then amplifies the padlock probe using RCA[4,5].

Innovation of single-molecule RNA imaging continues to build on smFISH and RCA-FISH to further improve detection efficiency, increase brightness and reduce overall cost. RNAscope leverages multiple tiled primary, secondary and tertiary DNA oligonucleotide probes[6]. Similarly, click-amplifying FISH (clampFISH) iteratively hybridizes padlock probes to target mRNAs and ligates them using bio-orthogonal click chemistry before hybridization with a FISH probe, resulting in a >400-fold signal amplification per single molecule of RNA[7]. Rather than tiling probes along a transcript, hybridization chain reaction (HCR)-FISH[8] and signal amplification by exchange reaction (SABER)-FISH[9] amplify primary probes with hairpin probes and concatemers, respectively, to tile fluorescent secondary probes along a primary probe. Other groups have made smFISH more cost-effective (smiFISH)[10] or have enabled the detection of single-nucleotide variants (SNVs) on transcripts (SNV FISH)[11] or adenosine-to-inosine-edited transcripts (inoFISH)[12].

Fixed-cell, multiplexed RNA imaging.

Subcellular multiplexed RNA imaging methods generally fall into two categories: combinatorial FISH and in situ sequencing.

Combinatorial FISH.—Combinatorial FISH assigns each unique RNA target a ‘spectral barcode’, with each bit in the barcode corresponding to a specific fluorochrome in a specific round of imaging. Increasing the number of bits in a barcode exponentially scales the number of unique transcripts that can be detected. In 2002, five pseudocolours and two rounds of imaging were leveraged to image ten unique transcripts[13]. In 2014, sequential FISH (seqFISH) used four colours and two rounds of imaging to detect 12 unique transcripts in budding yeast[14]. The advent of multiplexed error-robust FISH (MERFISH)

represented the first time the combinatorial labelling of RNA had pushed beyond 100 unique transcripts[15].

Subsequent developments to MERFISH[16] and seqFISH[14,17] both enable the detection of 10,000 unique RNA targets, but differ in how they address the challenge of optical crowding. Whereas MERFISH leverages expansion microscopy (ExM)[18], seqFISH+ opts for a sparse labelling approach[17] by detecting a small fraction of targets at each round of imaging.

In situ sequencing.—In 2013, in situ sequencing (ISS)[19] leveraged RCA-FISH and sequencing-by-ligation (SBL) to amplify and read out the barcode and identify the location of target mRNA. With modifications in probe design leading to a new barcoding system, the next iteration of ISS, hybridization-based ISS (HybISS), provided improved spatial detection of RNA transcripts[20]. BaristaSeq[21] followed a similar strategy but used Illumina sequencing-by-synthesis (SBS) chemistry. Recently, STARmap[22] increased the fidelity of ISS by using two partially complementary probes to label each target, a new error-robust SBL scheme (SEDAL) to sequence 5-nt barcodes, and hydrogel embedding to remove background autofluorescence. These advances enable STARmap to measure 1,020 genes simultaneously in intact medial prefrontal cortex tissue with an error rate of only ~1.8%.

Fluorescent in situ RNA sequencing (FISSEQ)[23,24] attempted the unbiased single-molecule measurement of all RNAs. Rather than hybridization with a padlock probe, FISSEQ hybridizes random hexamer primers. After reverse transcription, the cDNA itself is circularized using CircLigase II, becoming a template for RCA. Using SOLiD sequencing, the cDNA is partially sequenced and aligned to the genome. Although the unbiased measurement of the whole transcriptome was a major technical advancement, optical crowding, dominance of rRNA in resulting reads, and low circularization efficiency remain substantial hurdles to its widespread adoption. Expansion sequencing (ExSeq) addressed some of these limitations by pairing FISSEQ with ExM and ex situ sequencing to improve the overall detection efficiency and fidelity[25].

A promising new front in the battle of multiplexed RNA imaging methods is the use of RNA captured on spatially barcoded slides. The recently developed Seq-Scope repurposes Illumina next-generation sequencing (NGS) chemistry to generate clusters from captured RNAs with a distance of 0.5–0.8 μm between clusters[26]. Table 1 compares current methods of RNA imaging in fixed cells.

Live-cell, exogenous RNA imaging.

Fluorescently labelled RNA.—In 1997, Glotzer and colleagues microinjected fluorescently labelled *oskar* RNA into *Drosophila* oocytes to study its short-range and long-range transport[27]. Using similar strategies, microtubule-dependent transport of other RNAs in *Drosophila* oocytes, including *wingless* and *bicoid*, was also examined[28,29]. A drawback with microinjected RNA is the susceptibility to endosome entrapment[30].

RNA stem-loop systems.—In 1998, Singer and colleagues developed the RNA stem-loop system to visualize *ASH1* mRNA localized to the bud tip in *Saccharomyces cerevisiae*[31]. This system consists of two plasmids. One plasmid encodes a green fluorescent

protein (GFP) fused to the coding sequence for a single-stranded RNA phage capsid protein MS2, also called MS2 coat protein (MCP). The second plasmid expresses a reporter RNA containing the coding sequence of a protein of interest followed by six MS2 binding sites (MBSs). In 2003, single-molecule resolution of the MS2 system using 24 MBSs was demonstrated[32]. Several improvements on the first generation of MS2 have been developed to (1) overcome deletion of repetitive MS2 sequences[33], (2) improve the degradation and turnover of reporter mRNA carrying MS2[34], (3) enhance the signal-to-noise ratio and uniformity of RNA labelling[33] and (4) reduce background caused by unbound fluorescent protein by using split fluorescent protein or split Halotag[35–37]. Besides MS2, other RNA stem-loop systems have also emerged, including PP7, λ_{N22}, U1A and BglG[38–42]. In these systems, the stem-loop length varies from 15 to 29 nucleotides with their protein binding partners' sizes ranging from 22 to 129 amino acids[43]. The MS2/PP7 systems are relatively resistant to photobleaching as there are 48 GFPs on each mRNA, enabling RNA tracking to study the dynamics of mRNA processing[32,44]. Furthermore, the MS2 system could be genetically integrated into endogenous genes to study mRNA dynamics in live mouse brain tissue[45].

Fluorogenic RNA.—In 2011, Jaffrey and colleagues reported an RNA aptamer that mimics GFP[46]. In GFP, the three residues Ser[65]-Tyr[66]-Gly[67] form a fluorophore structure, 4-hydroxybenzlidene imidazolinone (HBI). Based on this principle, the authors performed systematic evolution of ligands by exponential enrichment (SELEX) and found an RNA aptamer, named Spinach, that can encase HBI, leading to fluorescence. To overcome the thermal instability and misfolding of Spinach, Spinach 2 was developed[47]. Following similar SELEX approaches for different fluorophores, other fluorogenic RNA systems, such as Broccoli, Mango, Pepper and Peach, have been engineered[48–51]. Recently, based on the bright and thermodynamically stable Mango aptamer, the Mango II array with 24 repeats of the aptamer sequence has been shown to achieve single-molecule resolution for live-cell RNA imaging[52].

Live-cell, endogenous RNA imaging.

All three systems, fluorescently labelled RNA, RNA stem-loop and fluorogenic RNA, are among the earliest methods developed to visualize RNA in living cells and have elucidated multiple aspects of RNA biology. One drawback of these systems is the inability to image endogenous, non-genetically modified mRNA. Chemically synthesized probes and genetically encoded probes are alternatives that can overcome this limitation.

Chemically synthesized probes.—In 1996, Tyagi and Kramer invented a single-stranded oligonucleotide probe, named 'molecular beacon', that fluoresces upon hybridization to target RNA[53]. Despite being proposed in the 1996 report that molecular beacon was suitable for RNA imaging in live cells[53], it was not until 2003 that this capability was demonstrated[54]. To overcome their instability in living cells, multiple chemistry modifications have been applied to molecular beacons, including 2′-*O*-methylribonuclotides, phosphorothioate backbones and locked nucleic acids[55]. In 2018, molecular beacon was shown to image endogenous RNA in living neurons with single-molecule resolution[56].

Another system that visualizes endogenous RNA involves incorporating fluorescently labelled dUTP into RNA during RNA synthesis. Typically, fluorescently labelled dUTPs are injected into early-stage embryos. RNAs with incorporated dUTPs are imaged in neurons differentiated from these embryos either in vitro or in vivo[57–59]. A limitation of this system is the inability to track specific RNA, as fluorescently labelled dUTP can integrate into any RNA.

Genetically encoded probes.—Following the discovery of clustered regularly interspaced short palindromic repeats (CRISPR) and CRISPR-associated (Cas) proteins that target DNA, it was found that in vitro programmable targeting of RNA is possible with Cas9 (RCas9)[60]. RCas9 can target RNA when the protospacer adjacent motif (PAM) sequence is provided *in trans* as a separate DNA oligonucleotide. In 2016, our laboratory demonstrated that RNA tracking in live cells was possible with RCas9 fused to a GFP[61]. In 2017, Zhang and colleagues showed that Cas13a can be engineered to target mammalian RNA and demonstrated live-cell RNA imaging with catalytically inactive Cas13a (dCas13a) fused to GFP[62]. A recent study in 2019 has compared the ability of multiple dCas13 proteins to image RNA in living cells and provide an improved signal-to-noise ratio by incorporating multiple fluorescent proteins into a single dCas13 protein[63]. Despite these efforts to engineer Cas systems for live-cell RNA imaging, single-molecule resolution has yet to be achieved. Table 1 compares current methods of live-cell RNA imaging.

RNA biology gained via imaging technologies

The advances in RNA imaging described above have increased our understanding of RNA throughout its functional life-cycle: transcription, splicing, localization, translation and degradation (Fig. 2).

Transcription.

Live-cell RNA imaging with MS2 systems can examine multiple transcriptional properties. For example, it has been used to describe transcriptional bursting[64,65]. A combination of fluorescently tagged RNA polymerase II and MS2 labelling of nascent mRNA has been applied to measure the elongation rate[66]. High-speed time-series measurements were able to discern elongation rate as well as observe multi-scale transcriptional bursting controlled via groups of closely spaced polymerases, termed ‘convoys’[67]. MS2-based bursting measurements from a single gene have been achieved using fluorescence fluctuation microscopy[68]. In vivo detection of transcriptional bursting was also demonstrated in acute brain slices from transgenic mice with 24 repeats of MS2 binding sites inserted into the β-actin gene[45]. MS2 systems have also been used to correlate the binding of Gal4 transcription factor to chromatin with transcriptional bursting[69].

Fluorescently labelled dUTPs combined with fluorescence anisotropy imaging have shown that chromatin structures are more open at transcriptionally active compartments in living cells[70]. Recently, MERFISH and seqFISH+ have been modified to study how chromosome three-dimensional (3D) organization affects transcriptional activity. seqFISH+ was modified to target the intronic regions of 10,421 genes and uncovered that nascent transcription sites were localized to the surfaces of chromosomes[71]. DNA-MERFISH was developed to trace

chromatin itself at the genome scale. A combination of DNA-MERFISH, MERFISH and immunofluorescence has simultaneously imaged over 1,000 gene loci, nascent transcripts from these loci and nuclear structures (nuclear speckles and nucleoli)[72].

Subcellular RNA imaging may continue to answer critical questions in transcription. The combined progress in live-cell RNA imaging at transcription sites and chromosomal architecture imaging with MERFISH and seqFISH+ may make headway towards understanding the mechanism of transcriptional bursting. The use of pooled genomic screens in concert with RNA imaging[73] can assess the contribution of different transcriptional activators and repressors.

Splicing.

In the early 1990s, following the finding that ~90% of pre-mRNAs are spliced during or after transcription[74], the next quest was to decipher the structural and kinetic coupling of splicing and transcription. Using smFISH, Tyagi and colleagues found that, when the intronic polypyrimidine tract is present within a strong secondary structure, splicing is uncoupled from transcription and delayed until transcription is completed[75]. Using live-cell RNA imaging with the MS2 system in combination with fluorescence recovery after photobleaching (FRAP), Shav-Tal and colleagues showed that splicing events do not affect polymerase elongation kinetics[76]. Using the MS2 system, it was shown that transcription is the rate-limiting step for the excision of long introns[77]. Combining MS2 and PP7 systems, Larson et al. labelled the introns with one fluorescent colour and the exons with another fluorescent colour to track transcription and splicing events simultaneously, and found that the two processes are coordinated via kinetic competition[78]. These studies have also shown that splicing occurs at variable timescales from 20 s to minutes. Furthermore, when quantifying at the level of a single cell, alternative splicing seems to occur stochastically, exhibiting cell-to-cell variability[79].

Transcriptomic studies have suggested alternative splicing as a mechanism for RNA localization[80,81]. Recently, APEX-seq, developed by Ting and colleagues, has further pushed the spatial resolution of transcriptome-wide mapping of isoforms by enabling the mapping of RNA localization to nine different organelles[82]. In highly asymmetric cells like neurons, where RNA localization along the neurites is linked to precise function, an even higher spatial resolution of transcriptome mapping will help to understand the precise role of alternative splicing in subcellular localization.

RNA transport.

The first study using an RNA stem-loop imaging system showed that ASH1 mRNA exhibited bidirectional movement with occasional stalling in yeast and reported that the transport speed ranged from 200 to 400 nm s^{-1}, consistent with the speed of the myosin V motor[31]. In mammalian systems, Arc mRNA appeared to travel at 0.1–1 μm s^{-1} (ref.[83]). Tracking RNA movement in *Cos* cells revealed four types of mobility with different probability: (1) immobility (33–40%), (2) directional movement (2–5%), (3) restricted diffusion (40–45%) and (4) diffusion (15–25%). Interestingly, mRNA can dynamically switch from one type of mobility to another[32].

RNAs synthesized within the nucleus exit through the nuclear pore complex (NPC) for further processing. Both the MS2 system[84] and molecular beacon[84] showed that ribonucleoprotein (RNP) complexes follow a diffusional model in the nucleus. mRNA export through the NPC appeared to be faster than a simple diffusion model based on imaging with the MS2 system[85]. Consistently, nucleocytoplasmic transport was found to follow a three-step model consisting of (1) docking (80 ms), (2) transport (5–20 ms) and (3) release (80 ms), in which transport through NPC was not the rate-limiting step. This finding was made possible using the MS2 system in combination with a super-registration approach capable of resolving 20-ms time precision and 26-nm spatial resolution[86].

Although previous studies suggested that multiple mRNA species can be packaged and transported within the same RNP[87–89], a study using smFISH and quantitative imaging showed that mRNA molecules travelled singly in neuronal dendrites[90]. A similar observation was made using a molecular beacon, which revealed that more than 70% of β-actin mRNA molecules travelled singly in neuronal axons[56]. This study also teased out different transport models in axons, including (1) diffusion and entrapment, (2) directed transport by motor proteins, (3) localized protection of mRNA from degradation and (4) a ‘sushi belt’ model that incorporates directed transport with local entrapment at synapses.

RNAs are thought to be packaged into RNPs for transport. However, the composition of RNPs and the process of packaging remain unclear. Further investigations are required to figure out the biological rules that govern RNP packaging, such as identification of the RNA-binding protein (RBP) required for packaging and transporting a given RNA. After being packaged, transport RNPs are thought to be shuffled to their destination by motor proteins via microtubes[91]. The adaptors connecting RNPs and motor proteins remain unknown. A recent study suggests that RNPs can attach to the lysosome for long-distance transport[92]. To what extent this mode of transportation applies to the transcriptome requires future studies. It has been suggested that mRNA molecules travel singly in neuronal dendrites and axons[56,89]. These studies, however, are limited to a small number of RNA species. Transporting a single mRNA at a time could guarantee specificity, although it appears to cost more energy than transporting multiple mRNAs at once to the same destination. A transcriptome-wide effort could give more insights into the universality of this process.

RNA localization.

The influence of subcellular RNA localization on cellular functions in a variety of cell types has been extensively reviewed[93–97]. Here we briefly discuss critical findings in the context of the advancement of subcellular RNA imaging technology.

In 1986, Singer and Lawrence were the first to establish distinct localization patterns of actin, vimentin and tubulin mRNAs in intact somatic cells via ISH[98]. Following this initial study, multiple investigations into the subcellular localization of individual mRNA species were conducted using smFISH[99–102]. Recently, MERFISH was performed to interrogate the subcellular localization of transcripts from ~10,000 genes[16]. As a validation, transcripts from gold-standard secretome genes were found to be enriched in the endoplasmic

reticulum[16]. Furthermore, the authors developed a pseudotime method based on nuclear/cytoplasmic RNA enrichment to indicate the cell-cycle state of individual cells.

Highly asymmetric cells such as neurons leverage localized translation to respond to stimuli with low latency. Local translation of β-actin mRNA following glutamate uncaging was demonstrated by a combination of FISH and a HaloTag-actin reporter construct to measure actin transcripts and proteins in dendritic spines[103]. Similarly, smFISH demonstrated that intestinal epithelia cells leverage asymmetric subcellular localization to polarize translational efficiency[104]. In axons, fluorescent-UTP labelling and SunTag nascent protein labelling were used to demonstrate that Rab7a endosomes carrying mRNA and ribosomes pause on mitochondria to translate mRNAs encoding mitochondrial proteins while traversing axons[57]. Even within non-polarized cells, mRNA localization was found to depend on ongoing local translation, suggesting co-translational RNA targeting[105].

RNA mislocalization has been implicated in multiple neurodegenerative diseases[106], and transcriptomic sequencing studies have identified those mislocalized mRNAs. The advent of spatial transcriptomics and live-cell RNA imaging equips us with the ability to study mRNA mislocalization at higher spatial and temporal resolution.

Translation.

Using translating RNA imaging by coat protein knock-off (TRICK), a double labelling of PP7 in the coding sequence and MS2 in 3′UTR, Chao and colleagues observed that mRNAs are not translated in the nucleus, but are translated within minutes of export[107]. Dual labelling of translating protein and RNA via SunTag and MS2 was used to understand translation in sub-dendrites[108], the number of ribosomes per polysome[109], as well as how ribosome occupancy decompacts mRNA[110]. Furthermore, the SunTag/MS2 strategy has enabled the discoveries that mRNAs resume translation during recovery from stress[111] and that mRNAs are translated in stress granules, arguing against a direct role of stress granules in the inhibition of protein synthesis[112].

Whereas live-cell imaging enables an understanding of the temporal dynamics of translation, fixed-cell RNA imaging allows the study of translation dynamics at a broader scale. A combination of smFISH and nascent protein staining by *O*-propargyl-puromycin revealed that global mRNA localization in the intestinal epithelium is polarized, which leads to a polarization in translational efficiency[104]. A similar approach has shown that mRNA localization requires ongoing translation, leading to widespread co-translational RNA targeting[105].

RNA degradation.

Using smFISH, Singer and colleagues studied cell-cycle-regulated RNA degradation in yeast and found that promoter-dependent activity directly influences how and when an mRNA will be degraded in the cytoplasm[113]. To study mRNA degradation at higher temporal resolution in living cells, Chao and colleagues developed a technique called 3′-RNA end accumulation during turnover (TREAT)[114], which utilizes a fluorescent reporter that leverages the orthogonality of MS2 and PP7 systems to label intact and degraded mRNAs. Using TREAT, they found that, unlike for transcription, mRNA degradation does

not burst. By labelling processing bodies (P-bodies) simultaneously with TREAT, they found that a majority of TREAT mRNAs are not degraded in P-bodies. This provides a new understanding of P-bodies, which were previously considered to be the centre of RNA degradation[115]. Furthermore, mRNAs localized to stress granules and P-bodies when exposed to stress showed no difference in degradation dynamics during recovery compared with cytosolic mRNAs[111].

In addition to the degradation of normal transcripts, cells have developed nonsense-mediated decay (NMD) to eliminate transcripts harbouring a premature termination codon. Imaging translating mRNA with the MS2/SunTag system[116] showed that NMD efficiency is affected by the number of introns and that, for the same RNA, each round of translation has an equal probability of inducing NMD[117].

Besides active transport and diffusive models, degradation has been proposed as a mechanism to induce and maintain RNA localization[118]. mRNAs transported in RNPs are typically protected from degradation, ensuring proper delivery to their destination. Future studies with high spatial and temporal resolution will shed light on the interplay between RNA degradation and localization.

ncRNA.

Even though more than 85% of the genome is transcribed to RNA[119], only <2% of the mammalian genome encodes proteins[120]. Hence, a majority of transcribed RNAs are ncRNAs, such as microRNAs (miRNAs) and long ncRNAs (lncRNAs). Intracellular single-molecule, high-resolution localization and counting (iSHiRLoC) has been developed to track the localization of microinjected fluorescently labelled miRNAs in living HeLa and U2OS cells[121–124] and revealed two kinetically distinct pathways of miRNA assembly into large RNPs[121]. iSHiRLoC also showed that miRNA stability and nuclear retention were dependent on Argonaute (Ago) proteins and targets. Furthermore, miRNA unwinding, strand selection and cytoplasmic retention were dependent on Ago2[123]. iSHiRLoC, together with tracking of fluorescently labelled P-bodies, revealed that miRNAs localized to P-bodies are mostly dysfunctional[124].

An smFISH survey on the localization of 61 lncRNAs found that nearly half exist in the cytoplasm[125]. For those lncRNAs that localize in the nucleus, their distribution can be either diffuse, in foci or in speckles and paraspeckles, like MALAT1 and NEAT1, respectively. Live-cell imaging of NEAT1 using dCas13-GFP showed that paraspeckles underwent ‘kiss-and-run/fusion’ dynamics, where materials rapidly moved in and out of paraspeckles[63]. smFISH revealed that lncRNAs exhibit cell-to-cell expression variability[125], like mRNAs. smFISH also showed that imprinting lncRNAs Kcnqlot1[126] and Air[127] localized at their target sites of transcription on the same allele, suggesting that these lncRNAs may silence their target genes *in cis*.

Viral RNA.

The human immunodeficiency virus (HIV) is one of the most well-studied RNA viruses. A study using the RNA stem-loop system and live-cell imaging found that more than 90% of HIV-1 particles contain viral RNA[38]. By labelling individual RNA strands with different

colours, it further showed that the HIV-1 structural protein Gag packages a dimeric RNA molecule, not two monomeric RNA molecules. Simultaneous imaging of the Gag protein and HIV-1 genome RNA has uncovered their dynamics and functional interactions during viral particle assembly at the plasma membrane[128]. The MS2/SunTag system shows that ~50% of HIV-1 RNA is actively translated and that Gag only packages non-translating RNA[129].

RNA imaging methods such as FISH and RNAscope have also been applied to detect the presence of viruses[130] and SARS-CoV-2[131–133], a single-stranded RNA virus that led to the COVID-19 pandemic with over six million fatalities worldwide. smFISH has been applied to visualize host mRNA dynamics during SARS-CoV-2 infection, revealing that the biogenesis of interferon (IFN) I and II, a marker of immune responses, is inhibited at multiple stages, including transcription induction, transcription release and nuclear-cytoplasmic transport of IFN mRNAs[134]. smFISH also confirms that activation of the cellular oxygen-sensing pathway inhibit SARS-CoV-2 entry and replication in lung epithelial cells[135].

outlook

As mRNA imaging in fixed cells has evolved from a single target to the transcriptome scale, imaging speed and image analysis have remained bottlenecks to the study of subcellular mRNA localization. Furthermore, the ability to resolve multiple mRNAs as diffraction-limited spots has become a challenge, inhibiting our understanding of whether different species of mRNA can be co-processing in the same place. Efforts in artificial intelligence to automate cell segmentation, RNA location assignment and spot detection and tracking will further push the boundary of our current understanding of RNA localization[101,136–138]. Going beyond expanding the number of mRNA species, the ability to image endogenous small RNAs, such as miRNA, and RNA isoforms will greatly enhance our understand of RNA biology at subcellular resolution.

The current live-cell RNA imaging methods have provided a huge leap towards a high spatiotemporal understanding of multiple aspects of RNA processing. However, studies have been limited to a few mRNA species and relatively short-term tracking. Live-cell RNA imaging with Cas holds great promise by offering a flexible, easy-to-use system to target any endogenous gene in the transcriptome, although single-molecule resolution has yet to be seen. In addition, a future system with multiplexing capability can open the door to explore whether and how different RNA species are co-processed. A limitation to long-term single-molecule tracking in live-cell imaging has been phototoxicity. Future developments in systems to overcome this will enable tracking mRNA throughout its life-cycle.

In addition to RNA imaging, multiple RNA sequencing and computational methods have been developed to study subcellular RNA localization, including APEX-seq[82], RNA-GPS[80], LncLocator[139], RNALocate[140], iLoc-lncRNA[141], Axon-seq[142], CeFrac-seq[143] and RNATracker[144]. Methods that detect RBP targets, such as TRIBE[145,146] and STAMP[147], can potentially be adapted to study RNA subcellular localization. Although these methods do not have the high spatiotemporal resolution of RNA imaging, the ability to multiplex and sequence isoforms is unmatched by current RNA imaging methods. Slide-seq[148], Seq-

scope[26] and ExSeq[25] have pushed the limits of transcriptomic imaging from known targets to unbiased profiling. Future methods incorporating the power of both RNA imaging and sequencing will help us to make a big leap forward in RNA biology.

In the past, high-resolution imaging was often thought of as a low-throughput method and not suitable for high-throughput screening, in comparison to other fluorescent methods such as flow cytometry and the fluorescent microplate reader. However, innovations in optical instrumentation, automation and image analysis have added high-throughput capability into fluorescent imaging. High-throughput screens via protein imaging have expanded our understanding of gene and protein functions[73,149,150]. We expect that new methods enabling high-throughput screens via RNA imaging will further contribute to our knowledge of not just gene and protein functions, but also RNA functions.

Finally, RNA processing involves not only RNA but also DNA and proteins. Going beyond an RNA-centric outlook, combining RNA imaging with DNA and RBP imaging will greatly enhance our understanding of RNA biology, answering questions such as how chromosome organization affects gene expression and how RNPs form and organize. Furthermore, an integration with high-throughput screen studies such as large-scale RBP–RNA interactions and CRISPR screens will also expand our toolbox to explore the multidimensionality of RNA processing (Fig. 3).

Acknowledgements

G.W.Y. is supported by NIH grants nos. AI132122, HG011864, NS103172, EY029166, HG004659 and HG009889. This research was partially supported by an Allen Distinguished Investigator Award to G.W.Y., a Paul G. Allen Frontiers Group advised grant of the Paul G. Allen Family Foundation. P.L. is supported by Schmidt Science Fellows. We thank M. Huang and C. Mah for their critical reading of the manuscript.

References

1. Singer RH & Ward DC Actin gene expression visualized in chicken muscle tissue culture by using in situ hybridization with a biotinated nucleotide analog. Proc. Natl Acad. Sci. USA 79, 7331–7335 (1982). [PubMed: 6961411]
2. Femino AM, Fay FS, Fogarty K & Singer RH Visualization of single RNA transcripts in situ. Science 280, 585–590 (1998). [PubMed: 9554849]
3. Raj A, Bogaard P, van den Rifkin SA, van Oudenaarden A & Tyagi S Imaging individual mRNA molecules using multiple singly labeled probes. Nat. Methods 5, 877–879 (2008). [PubMed: 18806792]
4. Larsson C et al. In situ genotyping individual DNA molecules by target-primed rolling-circle amplification of padlock probes. Nat. Methods 1, 227–232 (2004). [PubMed: 15782198]
5. Larsson C, Grundberg I, Söderberg O & Nilsson M In situ detection and genotyping of individual mRNA molecules. Nat. Methods 7, 395–397 (2010). [PubMed: 20383134]
6. Wang F et al. RNAscope: a novel in situ RNA analysis platform for formalin-fixed, paraffin-embedded tissues. J. Mol. Diagnostics 14, 22–29 (2012).
7. Rouhanifard SH et al. ClampFISH detects individual nucleic acid molecules using click chemistry-based amplification. Nat. Biotechnol 37, 84–89 (2018).
8. Choi HMT et al. Programmable in situ amplification for multiplexed imaging of mRNA expression. Nat. Biotechnol 28, 1208–1212 (2010). [PubMed: 21037591]
9. Kishi JY et al. SABER amplifies FISH: enhanced multiplexed imaging of RNA and DNA in cells and tissues. Nat. Methods 16, 533–544 (2019). [PubMed: 31110282]

10. Tsanov N et al. smiFISH and FISH-quant—a flexible single RNA detection approach with super-resolution capability. Nucleic Acids Res 44, e165 (2016). [PubMed: 27599845]
11. Levesque MJ, Ginart P, Wei Y & Raj A Visualizing SNVs to quantify allele-specific expression in single cells. Nat. Methods 10, 865–867 (2013). [PubMed: 23913259]
12. Mellis IA, Gupte R, Raj A & Rouhanifard SH Visualizing adenosine-to-inosine RNA editing in single mammalian cells. Nat. Methods 14, 801–804 (2017). [PubMed: 28604724]
13. Levsky JM, Shenoy SM, Pezo RC & Singer RH Single-cell gene expression profiling. Science 297, 836–840 (2002). [PubMed: 12161654]
14. Lubeck E, Coskun AF, Zhiyentayev T, Ahmad M & Cai L Single-cell in situ RNA profiling by sequential hybridization. Nat. Methods 11, 360–361 (2014). [PubMed: 24681720]
15. Chen KH, Boettiger AN, Moffitt JR, Wang S & Zhuang X Spatially resolved, highly multiplexed RNA profiling in single cells. Science 348, aaa6090 (2015).
16. Xia C, Fan J, Emanuel G, Hao J & Zhuang X Spatial transcriptome profiling by MERFISH reveals subcellular RNA compartmentalization and cell cycle-dependent gene expression. Proc. Natl Acad. Sci. USA 116, 19490–19499 (2019). [PubMed: 31501331]
17. Eng C-HL et al. Transcriptome-scale super-resolved imaging in tissues by RNA seqFISH. Nature 568, 235–239 (2019). [PubMed: 30911168]
18. Wang G, Moffitt JR & Zhuang X Multiplexed imaging of high-density libraries of RNAs with MERFISH and expansion microscopy. Sci. Rep 8, 4847 (2018). [PubMed: 29555914]
19. Ke R et al. In situ sequencing for RNA analysis in preserved tissue and cells. Nat. Methods 10, 857–860 (2013). [PubMed: 23852452]
20. Gyllborg D et al. Hybridization-based in situ sequencing (HybISS) for spatially resolved transcriptomics in human and mouse brain tissue. Nucleic Acids Res 48, e112 (2020). [PubMed: 32990747]
21. Chen X, Sun Y-C, Church GM, Lee JH & Zador AM Efficient in situ barcode sequencing using padlock probe-based BaristaSeq. Nucleic Acids Res 46, e22 (2018). [PubMed: 29190363]
22. Wang X et al. Three-dimensional intact-tissue sequencing of single-cell transcriptional states. Science 361, eaat5691 (2018).
23. Lee JH et al. Highly multiplexed subcellular RNA sequencing in situ. Science 343, 1360–1363 (2014). [PubMed: 24578530]
24. Lee JH et al. Fluorescent in situ sequencing (FISSEQ) of RNA for gene expression profiling in intact cells and tissues. Nat. Protoc 10, 442–458 (2015). [PubMed: 25675209]
25. Alon S et al. Expansion sequencing: spatially precise in situ transcriptomics in intact biological systems. Science 371, eaax2656 (2021).
26. Cho C-S et al. Microscopic examination of spatial transcriptome using Seq-Scope. Cell 184, 3559–3572 (2021). [PubMed: 34115981]
27. Glotzer JB, Saffrich R, Glotzer M & Ephrussi A Cytoplasmic flows localize injected oskar RNA in *Drosophila* oocytes. Curr. Biol 7, 326–337 (1997). [PubMed: 9115398]
28. Wilkie GS & Davis I *Drosophila* wingless and pair-rule transcripts localize apically by dynein-mediated transport of RNA particles. Cell 105, 209–219 (2001). [PubMed: 11336671]
29. Cha BJ, Koppetsch BS & Theurkauf WE In vivo analysis of drosophila bicoid mRNA localization reveals a novel microtubule-dependent axis specification pathway. Cell 106, 35–46 (2001). [PubMed: 11461700]
30. Bao G, Rhee WJ & Tsourkas A Fluorescent probes for live-cell RNA detection. Annu. Rev. Biomed. Eng 11, 25–47 (2009). [PubMed: 19400712]
31. Bertrand E et al. Localization of ASH1 mRNA particles in living yeast. Mol. Cell 2, 437–445 (1998). [PubMed: 9809065]
32. Fusco D et al. Single mRNA molecules demonstrate probabilistic movement in living mammalian cells. Curr. Biol 13, 161–167 (2003). [PubMed: 12546792]
33. Wu B et al. Synonymous modification results in highfidelity gene expression of repetitive protein and nucleotide sequences. Genes Dev 29, 876–886 (2015). [PubMed: 25877922]
34. Tutucci E et al. An improved MS2 system for accurate reporting of the mRNA life cycle. Nat. Methods 15, 81–89 (2018). [PubMed: 29131164]

35. Park SY, Moon HC & Park HY Live-cell imaging of single mRNA dynamics using split superfolder green fluorescent proteins with minimal background. RNA 26, 101–109 (2020). [PubMed: 31641028]
36. Wu B, Chen J & Singer RH Background free imaging of single mRNAs in live cells using split fluorescent proteins. Sci. Rep 4, 3615 (2014). [PubMed: 24402470]
37. Shao S et al. TagBiFC technique allows long-term single-molecule tracking of protein-protein interactions in living cells. Commun. Biol 4, 378 (2021). [PubMed: 33742089]
38. Chen J et al. High efficiency of HIV-1 genomic RNA packaging and heterozygote formation revealed by single virion analysis. Proc. Natl Acad. Sci. USA 106, 13535–13540 (2009). [PubMed: 19628694]
39. Takizawa PA & Vale RD The myosin motor, Myo4p, binds Ash1 mRNA via the adapter protein, She3p. Proc. Natl Acad. Sci. USA 97, 5273–5278 (2000). [PubMed: 10792032]
40. Wu B, Buxbaum AR, Katz ZB, Yoon YJ & Singer RH Quantifying protein-mRNA interactions in single live cells. Cell 162, 211–220 (2015). [PubMed: 26140598]
41. Brodsky AS & Silver PA Pre-mRNA processing factors are required for nuclear export. RNA 6, 1737–1749 (2000). [PubMed: 11142374]
42. Daigle N & Ellenberg J λ_N-GFP: an RNA reporter system for live-cell imaging. Nat. Methods 4, 633–636 (2007). [PubMed: 17603490]
43. Bos TJ, Nussbacher JK, Aigner S & Yeo GW in Advances in Experimental Medicine and Biology Vol. 907, 61–88 (Springer, 2016). [PubMed: 27256382]
44. Hocine S, Raymond P, Zenklusen D, Chao JA & Singer RH Single-molecule analysis of gene expression using two-color RNA labeling in live yeast. Nat. Methods 10, 119–121 (2012). [PubMed: 23263691]
45. Park HY et al. Visualization of dynamics of single endogenous mRNA labeled in live mouse. Science 343, 422–424 (2014). [PubMed: 24458643]
46. Paige JS, Wu KY & Jaffrey SR RNA mimics of green fluorescent protein. Science 333, 642–646 (2011). [PubMed: 21798953]
47. Strack RL, Disney MD & Jaffrey SR A superfolding Spinach2 reveals the dynamic nature of trinucleotide repeat-containing RNA. Nat. Methods 10, 1219–1224 (2013). [PubMed: 24162923]
48. Wu J et al. Live imaging of mRNA using RNA-stabilized fluorogenic proteins. Nat. Methods 16, 862–865 (2019). [PubMed: 31471614]
49. Filonov GS, Moon JD, Svensen N & Jaffrey SR Broccoli: rapid selection of an RNA mimic of green fluorescent protein by fluorescence-based selection and directed evolution. J. Am. Chem. Soc 136, 16299–16308 (2014). [PubMed: 25337688]
50. Dolgosheina EV et al. RNA Mango aptamer-fluorophore: a bright, high-affinity complex for RNA labeling and tracking. ACS Chem. Biol 9, 2412–2420 (2014). [PubMed: 25101481]
51. Kong KYS, Jeng SCY, Rayyan B & Unrau PJ RNA Peach and Mango: orthogonal two-color fluorogenic aptamers distinguish nearly identical ligands. RNA 27, 604–615 (2021). [PubMed: 33674421]
52. Cawte AD, Unrau PJ & Rueda DS Live cell imaging of single RNA molecules with fluorogenic Mango II arrays. Nat. Commun 11, 1283 (2020). [PubMed: 32152311]
53. Tyagi S & Kramer FR Molecular beacons: probes that fluoresce upon hybridization. Nat. Biotechnol 14, 303–308 (1996). [PubMed: 9630890]
54. Bratu DP, Cha B-J, Mhlanga MM, Kramer FR & Tyagi S Visualizing the distribution and transport of mRNAs in living cells. Proc. Natl Acad. Sci. USA 100, 13308–13313 (2003). [PubMed: 14583593]
55. Tyagi S Imaging intracellular RNA distribution and dynamics in living cells. Nat. Methods 6, 331–338 (2009). [PubMed: 19404252]
56. Turner-Bridger B et al. Single-molecule analysis of endogenous β-actin mRNA trafficking reveals a mechanism for compartmentalized mRNA localization in axons. Proc. Natl Acad. Sci. USA 115, E9697–E9706 (2018). [PubMed: 30254174]
57. Cioni JM et al. Late endosomes act as mRNA translation platforms and sustain mitochondria in axons. Cell 176, 56–72 (2019). [PubMed: 30612743]

58. Wong HHW et al. RNA docking and local translation regulate site-specific axon remodeling in vivo. Neuron 95, 852–868 (2017). [PubMed: 28781168]
59. Piper M et al. Differential requirement of F-actin and microtubule cytoskeleton in cue-induced local protein synthesis in axonal growth cones. Neural Dev. 10, 3 (2015). [PubMed: 25886013]
60. O'Connell MR et al. Programmable RNA recognition and cleavage by CRISPR/Cas9. Nature 516, 263–266 (2014). [PubMed: 25274302]
61. Nelles DA et al. Programmable RNA tracking in live cells with CRISPR/Cas9 resource programmable RNA tracking in live cells with CRISPR/Cas9. Cell 165, 488–496 (2016). [PubMed: 26997482]
62. Abudayyeh OO et al. RNA targeting with CRISPR-Cas13. Nature 550, 280–284 (2017). [PubMed: 28976959]
63. Yang LZ et al. Dynamic imaging of RNA in living cells by CRISPR-Cas13 systems. Mol. Cell 76, 981–997 (2019). [PubMed: 31757757]
64. Chubb JR, Trcek T, Shenoy SM & Singer RH Transcriptional pulsing of a developmental gene. Curr. Biol 16, 1018–1025 (2006). [PubMed: 16713960]
65. Golding I, Paulsson J, Zawilski SM & Cox EC Real-time kinetics of gene activity in individual bacteria. Cell 123, 1025–1036 (2005). [PubMed: 16360033]
66. Darzacq X et al. In vivo dynamics of RNA polymerase II transcription. Nat. Struct. Mol. Biol 14, 796–806 (2007). [PubMed: 17676063]
67. Tantale K et al. A single-molecule view of transcription reveals convoys of RNA polymerases and multi-scale bursting. Nat. Commun 7, 12248 (2016). [PubMed: 27461529]
68. Larson DR, Zenklusen D, Wu B, Chao JA & Singer RH Real-time observation of transcription initiation and elongation on an endogenous yeast gene. Science 332, 475–478 (2011). [PubMed: 21512033]
69. Donovan BT et al. Live-cell imaging reveals the interplay between transcription factors, nucleosomes and bursting. EMBO J 38, e100809 (2019). [PubMed: 31101674]
70. Sinha DK, Banerjee B, Maharana S & Shivashankar GV Probing the dynamic organization of transcription compartments and gene loci within the nucleus of living cells. Biophys. J 95, 5432–5438 (2008). [PubMed: 18805931]
71. Shah S et al. Dynamics and spatial genomics of the nascent transcriptome by intron seqFISH. Cell 174, 363–376 (2018). [PubMed: 29887381]
72. Su JH, Zheng P, Kinrot SS, Bintu B & Zhuang X Genome-scale imaging of the 3D organization and transcriptional activity of chromatin. Cell 182, 1641–1659 (2020). [PubMed: 32822575]
73. Feldman D et al. Optical pooled screens in human cells. Cell 179, 787–799 (2019). [PubMed: 31626775]
74. Baurén G & Wieslander L Splicing of Balbiani ring 1 gene pre-mRNA occurs simultaneously with transcription. Cell 76, 183–192 (1994). [PubMed: 8287477]
75. Vargas DY et al. Single-molecule imaging of transcriptionally coupled and uncoupled splicing. Cell 147, 1054–1065 (2011). [PubMed: 22118462]
76. Brody Y et al. The in vivo kinetics of RNA polymerase II elongation during co-transcriptional splicing. PLoS Biol 9, 1000573 (2011).
77. Martin RM, Rino J, Carvalho C, Kirchhausen T & Carmo-Fonseca M Live-cell visualization of Pre-mRNA splicing with single-molecule sensitivity. Cell Rep 4, 1144–1155 (2013). [PubMed: 24035393]
78. Coulon A et al. Kinetic competition during the transcription cycle results in stochastic RNA processing. eLife 3, e03939 (2014). [PubMed: 25271374]
79. Waks Z, Klein AM & Silver PA Cell-to-cell variability of alternative RNA splicing. Mol. Syst. Biol 7, 506 (2011). [PubMed: 21734645]
80. Wu KE, Parker KR, Fazal FM, Chang HY & Zou J RNA-GPS predicts high-resolution RNA subcellular localization and highlights the role of splicing. RNA 26, 851–865 (2020). [PubMed: 32220894]
81. Mattioli CC et al. Alternative 3′UTRs direct localization of functionally diverse protein isoforms in neuronal compartments. Nucleic Acids Res 47, 2560–2573 (2019). [PubMed: 30590745]

82. Fazal FM et al. Atlas of subcellular RNA localization revealed by APEX-Seq. Cell 178, 473–490 (2019). [PubMed: 31230715]
83. Dynes JL & Steward O Dynamics of bidirectional transport of Arc mRNA in neuronal dendrites. J. Comp. Neurol 500, 433–447 (2007). [PubMed: 17120280]
84. Vargas DY, Raj A, Marras SAE, Kramer FR & Tyagi S Mechanism of mRNA transport in the nucleus. Proc. Natl Acad. Sci. USA 102, 17008–17013 (2005). [PubMed: 16284251]
85. Mor A et al. Dynamics of single mRNP nucleocytoplasmic transport and export through the nuclear pore in living cells. Nat. Cell Biol 12, 543–552 (2010). [PubMed: 20453848]
86. Grünwald D & Singer RH In vivo imaging of labelled endogenous B-actin mRNA during nucleocytoplasmic transport. Nature 467, 604–607 (2010). [PubMed: 20844488]
87. Carson JH et al. Multiplexed RNA trafficking in oligodendrocytes and neurons. Biochim. Biophys. Acta 1779, 453–458 (2008). [PubMed: 18442491]
88. Gao Y, Tatavarty V, Korza G, Levin MK & Carson JH Multiplexed dendritic targeting of α calcium calmodulin-dependent protein kinase II, neurogranin, and activity-regulated cytoskeleton-associated protein RNAs by the A2 pathway. Mol. Biol. Cell 19, 2311–2327 (2008). [PubMed: 18305102]
89. Tübing F et al. Dendritically localized transcripts are sorted into distinct ribonucleoprotein particles that display fast directional motility along dendrites of hippocampal neurons. J. Neurosci 30, 4160–4170 (2010). [PubMed: 20237286]
90. Batish M, Van Den Bogaard P, Kramer FR & Tyagi S Neuronal mRNAs travel singly into dendrites. Proc. Natl Acad. Sci. USA 109, 4645–4650 (2012). [PubMed: 22392993]
91. Rodrigues EC, Grawenhoff J, Baumann SJ, Lorenzon N & Maurer SP Mammalian neuronal mRNA transport complexes: the few knowns and the many unknowns. Front. Integr. Neurosci 15, 692948 (2021). [PubMed: 34211375]
92. Ya-Cheng Liao A et al. RNA granules hitchhike on lysosomes for long-distance transport, using annexin A11 as a molecular tether. Cell 179, 147–164 (2019). [PubMed: 31539493]
93. Medioni C, Mowry K & Besse F Principles and roles of mRNA localization in animal development. Development 139, 3263–3276 (2012). [PubMed: 22912410]
94. Kloc M, Zearfoss NR & Etkin LD Mechanisms of subcellular mRNA localization. Cell 108, 533–544 (2002). [PubMed: 11909524]
95. Engel KL, Arora A, Goering R, Lo H-YG & Taliaferro JM Mechanisms and consequences of subcellular RNA localization across diverse cell types. Traffic 21, 404–418 (2020). [PubMed: 32291836]
96. Fernandopulle MS, Lippincott-Schwartz J & Ward ME RNA transport and local translation in neurodevelopmental and neurodegenerative disease. Nat. Neurosci 24, 622–632 (2021). [PubMed: 33510479]
97. Thelen MP & Kye MJ The role of RNA binding proteins for local mRNA translation: implications in neurological disorders. Front. Mol. Biosci 6, 161 (2020). [PubMed: 32010708]
98. Lawrence JB & Singer RH Intracellular localization of messenger RNAs for cytoskeletal proteins. Cell 45, 407–415 (1986). [PubMed: 3698103]
99. Stoeger T, Battich N, Herrmann MD, Yakimovich Y & Pelkmans L Computer vision for image-based transcriptomics. Methods 85, 44–53 (2015). [PubMed: 26014038]
100. Samacoits A et al. A computational framework to study sub-cellular RNA localization. Nat. Commun 9, 4584 (2018). [PubMed: 30389932]
101. Petukhov V et al. Cell segmentation in imaging-based spatial transcriptomics. Nat. Biotechnol 40, 345–354 (2021). [PubMed: 34650268]
102. Battich N, Stoeger T & Pelkmans L Image-based transcriptomics in thousands of single human cells at single-molecule resolution. Nat. Methods 10, 1127–1133 (2013). [PubMed: 24097269]
103. Yoon YJ et al. Glutamate-induced RNA localization and translation in neurons. Proc. Natl Acad. Sci. USA 113, E6877–E6886 (2016). [PubMed: 27791158]
104. Moor AE et al. Global mRNA polarization regulates translation efficiency in the intestinal epithelium. Science 357, 1299–1303 (2017). [PubMed: 28798045]

105. Chouaib R et al. A dual protein-mRNA localization screen reveals compartmentalized translation and widespread co-translational RNA targeting. Dev. Cell 54, 773–791 (2020). [PubMed: 32783880]
106. Turner-Bridger B, Caterino C & Cioni JM Molecular mechanisms behind mRNA localization in axons: axonal mRNA localisation. Open Biol 10, 200177 (2020). [PubMed: 32961072]
107. Halstead JM et al. An RNA biosensor for imaging the first round of translation from single cells to living animals. Science 347, 1367–1671 (2015). [PubMed: 25792328]
108. Wu B, Eliscovich C, Yoon YJ & Singer RH Translation dynamics of single mRNAs in live cells and neurons. Science 352, 1430–1435 (2016). [PubMed: 27313041]
109. Morisaki T et al. Real-time quantification of single RNA translation dynamics in living cells. Science 352, 1425–1429 (2016). [PubMed: 27313040]
110. Adivarahan S et al. Spatial organization of single mRNPs at different stages of the gene expression pathway. Mol. Cell 72, 727–738 (2018). [PubMed: 30415950]
111. Wilbertz JH et al. Single-molecule imaging of mRNA localization and regulation during the integrated stress response. Mol. Cell 73, 946–958 (2019). [PubMed: 30661979]
112. Mateju D et al. Single-molecule imaging reveals translation of mRNAs localized to stress granules. Cell 183, 1801–1812 (2020). [PubMed: 33308477]
113. Trcek T, Larson DR, Moldón A, Query CC & Singer RH Single-molecule mRNA decay measurements reveal promoter-regulated mRNA stability in yeast. Cell 147, 1484–1497 (2011). [PubMed: 22196726]
114. Horvathova I et al. The dynamics of mRNA turnover revealed by single-molecule imaging in single cells. Mol. Cell 68, 615–625 (2017). [PubMed: 29056324]
115. Sheth U & Parker R Decapping and decay of messenger RNA occur in cytoplasmic processing bodies. Science 300, 805–808 (2003). [PubMed: 12730603]
116. Tanenbaum ME, Gilbert LA, Qi LS, Weissman JS & Vale RD A protein-tagging system for signal amplification in gene expression and fluorescence imaging. Cell 159, 635–646 (2014). [PubMed: 25307933]
117. Hoek TA et al. Single-molecule imaging uncovers rules governing nonsense-mediated mRNA decay. Mol. Cell 75, 324–339 (2019). [PubMed: 31155380]
118. Parton RM, Davidson A, Davis I & Weil TT Subcellular mRNA localisation at a glance. J. Cell Sci 127, 2127–2133 (2014). [PubMed: 24833669]
119. Hangauer MJ, Vaughn IW & McManus MT Pervasive transcription of the human genome produces thousands of previously unidentified long intergenic noncoding RNAs. PLoS Genet 9, e1003569 (2013). [PubMed: 23818866]
120. Carninci P Non-coding RNA transcription: turning on neighbours. Nat. Cell Biol 109, 1023–1024 (2008).
121. Pitchiaya S, Androsavich JR & Walter NG Intracellular single molecule microscopy reveals two kinetically distinct pathways for microRNA assembly. EMBO Rep 13, 709–715 (2012). [PubMed: 22688967]
122. Pitchiaya S, Krishnan V, Custer TC & Walter NG Dissecting non-coding RNA mechanisms in cellulo by single-molecule high-resolution localization and counting. Methods 63, 188–199 (2013). [PubMed: 23820309]
123. Pitchiaya S, Heinicke LA, Park JI, Cameron EL & Walter NG Resolving subcellular miRNA trafficking and turnover at single-molecule resolution. Cell Rep 19, 630–642 (2017). [PubMed: 28423324]
124. Pitchiaya S et al. Dynamic recruitment of single RNAs to processing bodies depends on RNA functionality. Mol. Cell 74, 521–533 (2019). [PubMed: 30952514]
125. Cabili MN et al. Localization and abundance analysis of human lncRNAs at single-cell and single-molecule resolution. Genome Biol 16, 20 (2015). [PubMed: 25630241]
126. Terranova R et al. Polycomb group proteins Ezh2 and Rnf2 direct genomic contraction and imprinted repression in early mouse embryos. Dev. Cell 15, 668–679 (2008). [PubMed: 18848501]

127. Nagano T et al. The Air noncoding RNA epigenetically silences transcription by targeting G9a to chromatin. Science 322, 1717–1720 (2008). [PubMed: 18988810]
128. Jouvenet N, Simon SM & Bieniasz PD Imaging the interaction of HIV-1 genomes and Gag during assembly of individual viral particles. Proc. Natl Acad. Sci. USA 106, 19114–19119 (2009). [PubMed: 19861549]
129. Chen J et al. Visualizing the translation and packaging of HIV-1 full-length RNA. Proc. Natl Acad. Sci. USA 117, 6145–6155 (2020). [PubMed: 32132202]
130. Shaffer SM et al. Multiplexed detection of viral infections using rapid in situ RNA analysis on a chip. Lab Chip 15, 3170–3182 (2015). [PubMed: 26113495]
131. Liu F et al. SARS-CoV-2 infects endothelial cells in vivo and in vitro. Front. Cell. Infect. Microbiol 11, 701278 (2021). [PubMed: 34307198]
132. Carossino M et al. Detection of SARS-CoV-2 by RNAscope® in situ hybridization and immunohistochemistry techniques. Arch. Virol 165, 2373–2377 (2020). [PubMed: 32761270]
133. Hepp C et al. Viral detection and identification in 20 min by rapid single-particle fluorescence in-situ hybridization of viral RNA. Sci. Rep 11, 19579 (2021). [PubMed: 34599242]
134. Burke JM, St Clair LA, Perera R & Parker R SARS-CoV-2 infection triggers widespread host mRNA decay leading to an mRNA export block. RNA 27, 1318–1329 (2021). [PubMed: 34315815]
135. Wing PAC, Keeley TP, Hodson EJ, Bishop T & Mckeating JA Hypoxic and pharmacological activation of HIF inhibits SARS-CoV-2 infection of lung epithelial cells. Cell Rep 35, 109020 (2021). [PubMed: 33852916]
136. Caicedo JC et al. Data-analysis strategies for image-based cell profiling. Nat. Methods 14, 849–863 (2017). [PubMed: 28858338]
137. Moen E et al. Deep learning for cellular image analysis. Nat. Methods 16, 1233–1246 (2019). [PubMed: 31133758]
138. Ronneberger O, Fischer P & Brox T U-Net: convolutional networks for biomedical image segmentation. Lect. Notes Comput. Sci 9351, 234–241 (2015).
139. Cao Z, Pan X, Yang Y, Huang Y & Shen H-B The lncLocator: a subcellular localization predictor for long non-coding RNAs based on a stacked ensemble classifier. Bioinformatics 34, 2185–2194 (2018). [PubMed: 29462250]
140. Zhang T et al. RNALocate: a resource for RNA subcellular localizations. Nucleic Acids Res 45, D135–D138 (2017). [PubMed: 27543076]
141. Su Z-D et al. iLoc-lncRNA: predict the subcellular location of lncRNAs by incorporating octamer composition into general PseKNC. Bioinformatics 34, 4196–4204 (2018). [PubMed: 29931187]
142. Nijssen J, Aguila J, Hoogstraaten R, Kee N & Hedlund E Axon-seq decodes the motor axon transcriptome and its modulation in response to ALS. Stem Cell Rep 11, 1565–1578 (2018).
143. Bouvrette LPB et al. CeFra-seq reveals broad asymmetric mRNA and noncoding RNA distribution profiles in *Drosophila* and human cells. RNA 24, 98–113 (2018). [PubMed: 29079635]
144. Yan Z, Lécuyer E & Blanchette M Prediction of mRNA subcellular localization using deep recurrent neural networks. Bioinformatics 35, i333–i342 (2019). [PubMed: 31510698]
145. McMahon AC et al. TRIBE: hijacking an RNA-editing enzyme to identify cell-specific targets of RNA-binding proteins. Cell 165, 742–753 (2016). [PubMed: 27040499]
146. Biswas J, Rahman R, Gupta V, Rosbash M & Singer RH MS2-TRIBE evaluates both protein-RNA interactions and nuclear organization of transcription by RNA editing. iScience 23, 101318 (2020). [PubMed: 32674054]
147. Brannan KW et al. Robust single-cell discovery of RNA targets of RNA-binding proteins and ribosomes. Nat. Methods 18, 507–519 (2021). [PubMed: 33963355]
148. Rodriques SG et al. Slide-seq: a scalable technology for measuring genome-wide expression at high spatial resolution. Science 363, 1463–1467 (2019). [PubMed: 30923225]
149. Wheeler EC et al. Pooled CRISPR screens with imaging on microraft arrays reveals stress granule-regulatory factors. Nat. Methods 17, 636–642 (2020). [PubMed: 32393832]

150. Markmiller S et al. Context-dependent and disease-specific diversity in protein interactions within stress granules. Cell 172, 590–604 (2018). [PubMed: 29373831]

151. Takei Y et al. Integrated spatial genomics reveals global architecture of single nuclei. Nature 590, 344–350 (2021). [PubMed: 33505024]

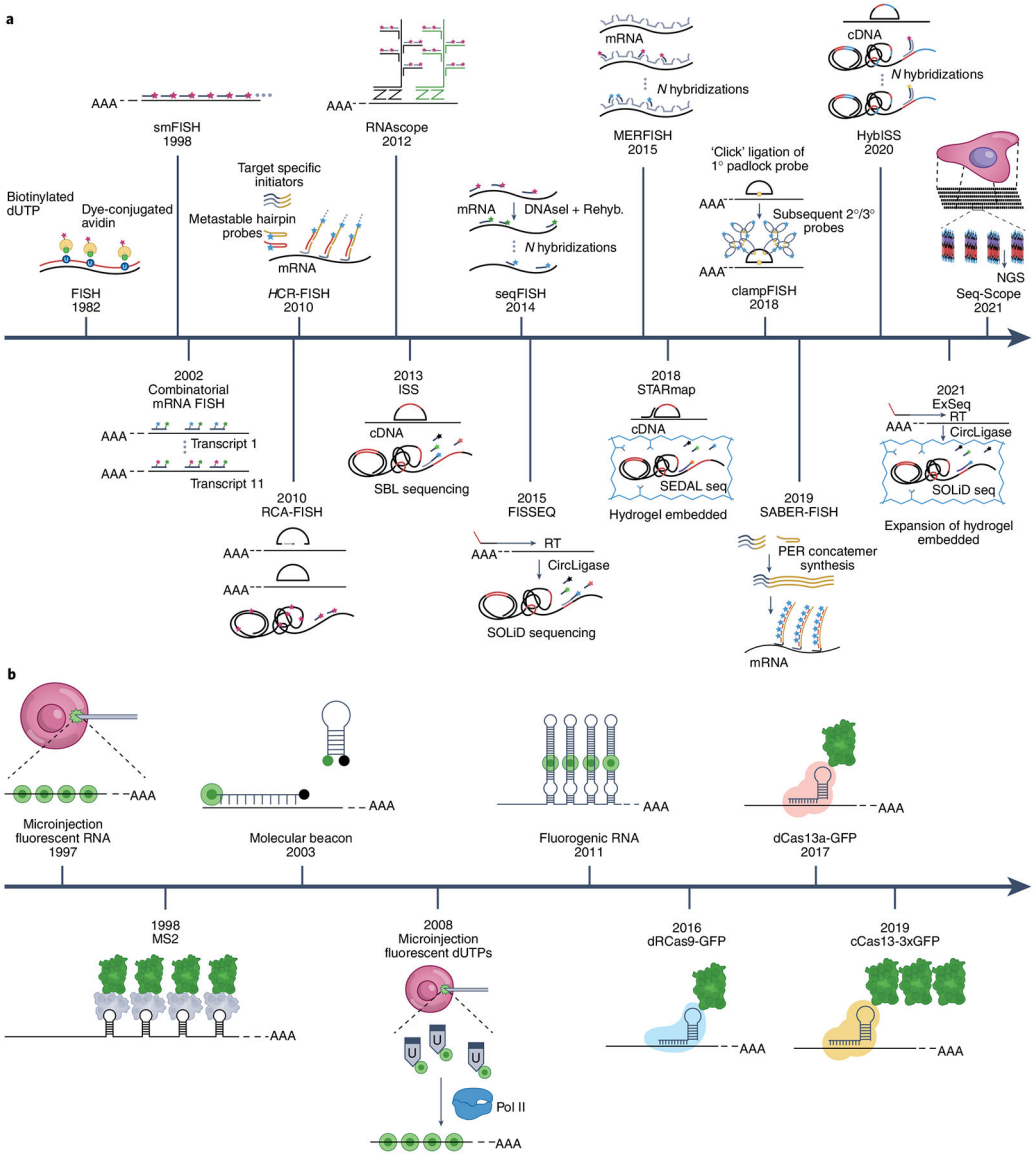

Fig. 1 |. Timeline of subcellular RNA imaging technologies.

a, The development of fixed-cell RNA imaging from the development of fluorescent RNA detection in 1982. smFISH amplifies signals by utilizing multiple fluorescent DNA probes binding to a single RNA target. RCA-FISH, clampFISH, HCR-FISH, RNAscope and SABER-FISH enhance signals by amplifying the primary probes that hybridize to the RNA target by RCA, by secondary and tertiary probes, or by primer-exchange reaction (PER). Fluorescently labelled DNA probes bind to these amplified sites and emit much brighter signals compared to smFISH. Combinatorial FISH methods (MERFISH, seqFISH) and in situ sequencing (ISS, FISSEQ, STARmap, HybISS, ExSeq, Seq-Scope) methods enable multiplexing. **b**, The evolution of live-cell RNA imaging started with the microinjection of fluorescent RNA in 1997. The stem-loop system takes advantage of a fluorescent protein attached to a viral coat protein that can bind to an RNA stem loop, such as MS2, enabling single-molecule resolution for the first time. The molecular beacon, which remains dark

until hybridized to a target RNA, can be delivered to cells to image endogenous RNA. Fluorogenic RNA takes advantage of an RNA aptamer that can encase the fluorophore structure 4-hydroxybenzylidene imidazolinone and emit light. Microinjected fluorescent dUTPs can be incorporated into endogenous RNA, enabling visualization. Recently, conjugates of fluorescent protein and RNA-binding Cas proteins were developed to visualize endogenous RNA in living cells. '*N* hybridizations' indicates *N* rounds of hybridizations; Rehyb., rehybridization.

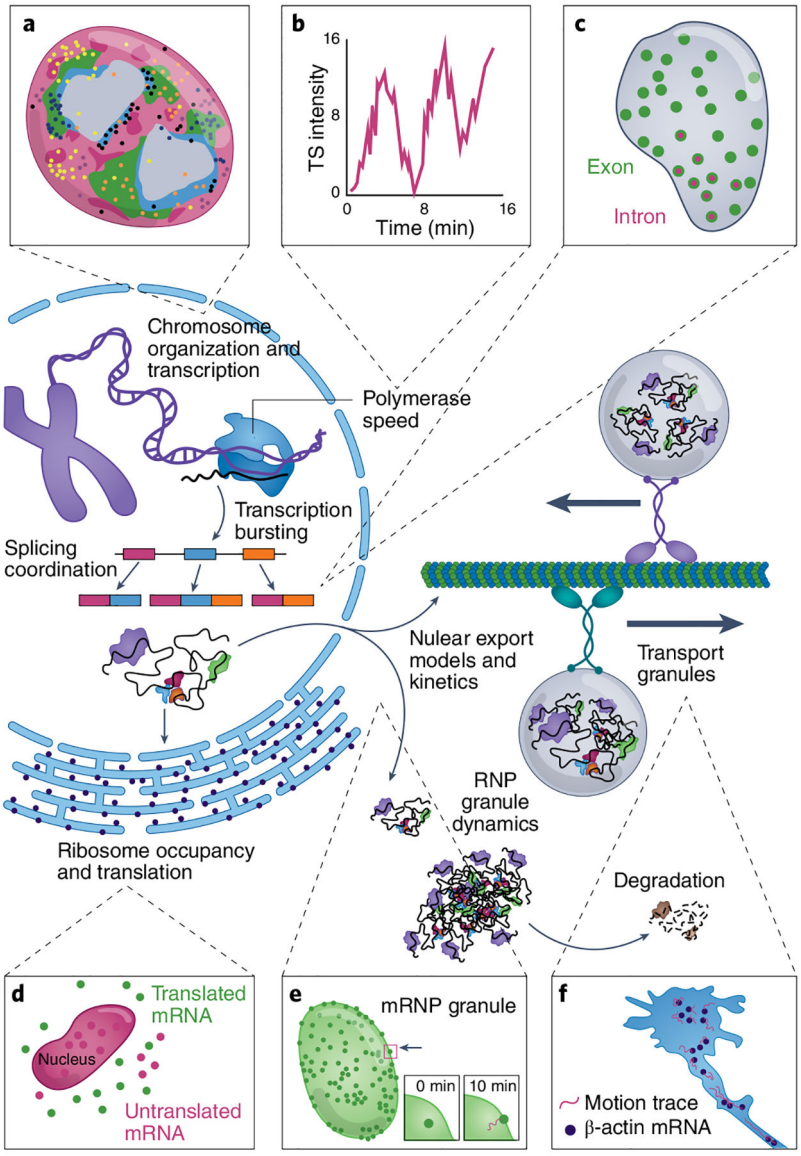

Fig. 2 |. Highlights of RNA biological insights gained through RNA imaging.

a, Multiplexed RNA imaging combined with chromatin tracing, such as with seqFISH+, can be used to elucidate nuclear domains with distinct chromatin states and gene expression[151]. **b**,**c**, Live-cell imaging using stem-loop systems can examine transcriptional properties such as bursting at transcription sites (TSs)[69] (**b**) and the temporal and spatial characteristics of splicing[75] (**c**). **d**, Stem-loop system and translating RNA imaging by coat protein knock-off (TRICK) assay revealed the dynamics of the initiation of protein synthesis on a single RNA[107]. **e**,**f**, Stem-loop systems can also be leveraged to track the dynamics of RNA nuclear export[85] (**e**) and RNA transport over time (**f**) in highly asymmetric cells such as neurons[56].

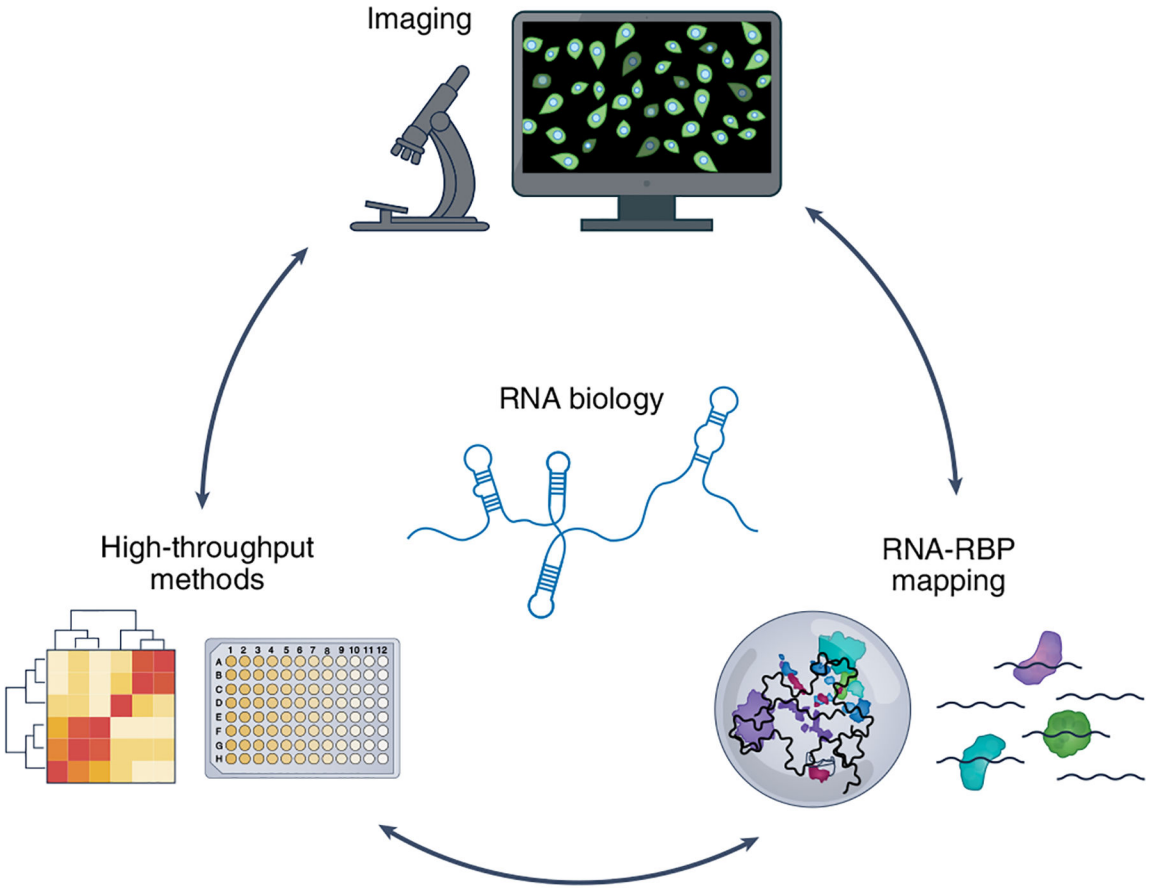

Fig. 3 |. The outlook towards a multidimensional approach to study RNA biology.
Integration of the high spatiotemporal approach of RNA imaging with high-throughput methods (such as RNA sequencing and the CRISPR screen) and large-scale RBP–RNA interaction mapping techniques to build a complete picture of RNA processing from RNA, DNA and protein perspectives.

Table 1 |

Current methods of RNA imaging

Method	Live/ fixed	Throughput	Error detection	Optical de-crowding	Isoform	RNA species specificity	Genetically modify	Single-molecule sensitivity	Detection of endogenous unmodified RNA	Commercial product	Ref.
smFISH	Fixed	Single gene per colour	No	Not needed	No	Yes	No	Yes	Yes	Stellaris	2–5
smiFISH	Fixed	Single gene per colour	No	Not needed	No	Yes	No	Yes	Yes	No	10
SNV FISH	Fixed	Single gene per colour	No	Not needed	Limited	Yes	No	Yes	Yes	No	11
inoFISH	Fixed	Single gene per colour	No	Not needed	Limited	Yes	No	Yes	Yes	No	12
HCR-FISH	Fixed	Single gene per colour	No	Not needed	Limited	Yes	No	Yes	Yes	Molecular Instruments	8
SABER-FISH	Fixed	10	No	Not needed	Limited	Yes	No	Yes	Yes	No	9
ClampFISH	Fixed	Single gene per colour	No	Not needed	Limited	Yes	No	Yes	Yes	No	7
RNAscope	Fixed	12	No	Not needed	No	Yes	No	Yes	Yes	ACD Bio	6
seqFISH+	Fixed	10,000	Yes	Sparse labelling	Limited	Yes	No	Yes	Yes	Spatial Genomics	17
MERFISH	Fixed	10,000	Yes	Expansion microscopy	Limited	Yes	No	Yes	Yes	Vizgen	15,16,18
STARmap	Fixed	1,000	Yes	None	No	Yes	No	Yes	Yes	No	22
HybISS	Fixed	119	Yes	Sparse labelling	No	Yes	No	Yes	Yes	Cartana (10x Genomics)	20
FISSEQ	Fixed	Whole transcriptome	No	Expansion microscopy	Yes	Yes	No	Yes	Yes	Readcoor (10x Genomics)	23–25
Fluorescently labelled RNA	Live	Single gene per colour	No	Not needed	No	Yes	No	No	No	No	27
RNA stem-loop system	Live	Single gene per colour	No	Not needed	No	Yes	Yes	Yes	No	No	31,32
Fluorogenic RNA	Live	Single gene per colour	No	Not needed	No	Yes	Yes	Yes	No	No	46,48,52
Molecular beacon	Live	Single gene per colour	No	Not needed	No	Yes	No	Yes	Yes	No	53,54,56

Method	Live/ fixed	Throughput	Error detection	Optical de-crowding	Isoform	RNA species specificity	Genetically modify	Single-molecule sensitivity	Detection of endogenous unmodified RNA	Commercial product	Ref.
Fluorescent dUTP	Live	Single gene per colour	No	Not needed	No	No	No	No	Yes	No	57,58,70
Cas system	Live	Single gene per colour	No	Not needed	No	Yes	Yes	No	Yes	No	61–63